

## FUSION BY DIFFUSION\*

W. J. ŚWIĄTECKI

Nuclear Science Division, Lawrence Berkeley National Laboratory  
Berkeley, California 94720, USA

K. SIWEK-WILCZYŃSKA

Institute of Experimental Physics, Warsaw University  
Hoża 69, 00-681 Warsaw, Poland

AND J. WILCZYŃSKI

The Andrzej Sołtan Institute for Nuclear Studies  
05-400 Otwock-Świerk, Poland

*(Received September 24, 2002)*

We present a theoretical interpretation of the cross sections to produce elements with atomic numbers  $Z = 102-118$ , in bombardments of a  $^{208}\text{Pb}$  target with projectiles ranging from  $^{48}\text{Ca}$  to  $^{86}\text{Kr}$ . The formation cross section is taken to be the product of three factors: the cross section for the projectile and target to stick, the probability for the resulting composite nucleus to reach the compound nucleus configuration by diffusion, and the probability for the latter to survive fission and to emit only one neutron. The first and third factors are treated according to more or less conventional formulae, whilst the middle one is based on the statistical (Brownian-like) diffusion of probability over a barrier in the form of an inverted parabola. The early dynamics of the neck growth is replaced by an assumption of a rapid injection into a macroscopically calculated asymmetric fission valley, after which the diffusion process begins. The measured cross sections can be reproduced fairly well by introducing an assumption about the separation between the surfaces of the approaching nuclei at which injection takes place. The optimum bombarding energies corresponding to the peaks of the excitation functions can be predicted by an elementary ‘optimum energy rule’, and the narrow widths of the measured excitation functions are readily accounted for.

PACS numbers: 24.60.Ky, 25.70.Jj

---

\* Presented at the XXXVII Zakopane School of Physics “Trends in Nuclear Physics”, Zakopane, Poland, September 3-10, 2002.

## 1. Introduction

Fig. 1 shows, on a logarithmic scale, experimental cross sections for producing a number of very heavy elements in bombardments of a lead target with projectiles ranging from  $^{48}\text{Ca}$  to  $^{86}\text{Kr}$  [1–4]. (In each case only one neutron was emitted from the compound nucleus.) One would like to have a theoretical understanding of these cross sections and be able to extrapolate the trends to other heavy systems. For experimentalists engaged in synthesizing heavy elements this is obviously important. Moreover, there is some instructive physics behind these numbers, which may be of general interest.

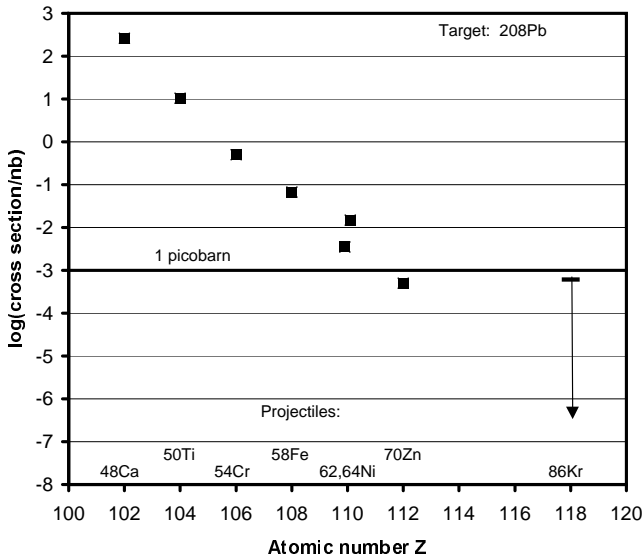


Fig. 1. Measured cross sections for the production of elements with atomic numbers  $Z$  in bombardments of a  $^{208}\text{Pb}$  target with the projectiles shown. The cross sections refer to the maxima of the Gaussian representations of the data in Fig. 19 of Ref. [1], supplemented by [2,3]. Except for the reactions with  $^{50}\text{Ti}$  and  $^{58}\text{Fe}$ , the cross sections are based on very few events at one, two or three bombarding energies, and are subject to considerable uncertainty. In the case of the compound nuclei  $^{270}110$  and  $^{272}110$ , the cross sections are displayed (here and in subsequent figures) at  $Z = 109.9$  and  $110.1$  in order to facilitate their identification. The upper limit for  $Z = 118$  is based on Ref. [4].

To bring this out, let me re-plot the above cross sections by dividing them by cross sections that would be expected on the basis of theories that work quite well for all but the heaviest systems. I will say more about these theories in Sections 5 and 6, but for now let me just note that they have two ingredients:

- (1) an estimate of the cross section  $\sigma_s$  for the colliding nuclei to stick, and
- (2) the probability  $P$  for the excited compound nucleus — *assumed to have been formed automatically after sticking* — to survive fission and emit exactly one neutron.

Using these ‘conventional’ ingredients we calculated the expected peak cross sections for the eight reactions under consideration. They are denoted by  $\sigma_{\text{con}}(\text{max})$  and listed in column 6 in Table I. Column 7 lists the measured or estimated cross sections, nominally at the maxima of the excitation functions, denoted by  $\sigma_{\text{exp}}(\text{max})$  [1–4]. Column 8 and Fig. 2 show the logarithm of the ratios  $\sigma_{\text{exp}}(\text{max})/\sigma_{\text{con}}(\text{max})$ , which I will refer to as ‘experimental’ hindrance factors,  $H$ . (Column 4 will be discussed later.) In the case of element 112 the hindrance  $H$  is some four and a half orders of magnitude. The trend, if extrapolated to the reaction  $^{86}\text{Kr} + ^{208}\text{Pb}$ , would suggest a further hindrance of about 100. What is the physics of these mysterious hindrances?

TABLE I

Peak cross sections and hindrance factors for  $1n$  reactions.

Projec- tile	$Z_{\text{CN}}$	$\sigma_s(\text{max})$ nb	$\Gamma_n/\Gamma_t$ $\times 10^5$	$P$ $\times 10^5$	$\sigma_{\text{con}}(\text{max})$ nb	$\sigma_{\text{exp}}(\text{max})$ nb	$\log H$
$^{48}\text{Ca}$	102	22,600	2983	2367	534.4	260	-0.313
$^{50}\text{Ti}$	104	32,100	640.4	543.3	174.3	10.4	-1.22
$^{54}\text{Cr}$	106	73,500	130.2	129.7	95.32	0.50	-2.28
$^{58}\text{Fe}$	108	194,000	21.16	16.31	31.68	0.067	-2.68
$^{62}\text{Ni}$	110	356,000	0.953	0.709	2.521	0.0035	-2.86
$^{64}\text{Ni}$	110	536,000	6.787	6.787	36.37	0.0150	-3.39
$^{70}\text{Zn}$	112	697,000	2.449	2.449	17.06	0.0005	-4.53
$^{86}\text{Kr}$	118	4,540,000	3.239	3.052	138.6	< 0.0006	< -5.36

I should not have said ‘mysterious’ because, qualitatively at least, it has been known since the eighties that the hindrance has to do with a simple geometrical feature of nucleus–nucleus collisions, namely the shrinking of the overall length of the fission saddle point shape with increasing atomic number  $Z$  [5–7]. For sufficiently heavy systems, the overall length of the saddle-point shape shrinks below the length of the entrance channel contact configuration (approximately equal to the sum of target and projectile diameters). Hence, after contact and the formation of a very heavy composite mononucleus, the system finds itself *outside rather than inside the above critical potential energy barrier*. As a result, *automatic fusion no longer takes place after contact*. The underlying physics is simply that the electrostatic repulsion has

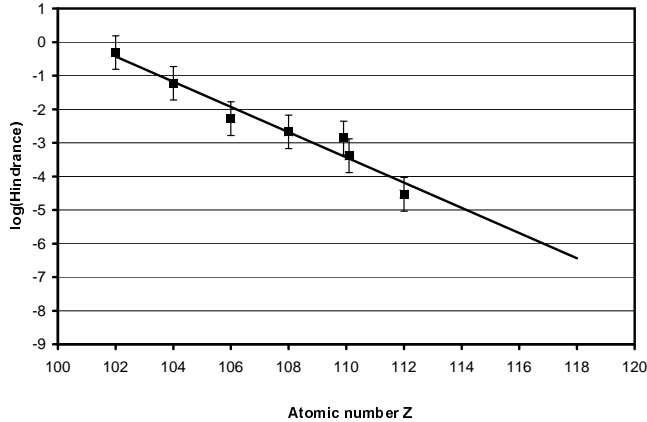


Fig. 2. Hindrance factors obtained by dividing the cross sections from Fig. 1 by peak cross sections obtained by taking the product of the sticking cross section from Eq. (7) and the survival probability from Eq. (11). The line is a fit to the points. Nominal error bars of half an order of magnitude are displayed in order to draw attention to both the experimental uncertainties in the data and to the limited accuracy of Eqs. (7) and (11).

become stronger than the nuclear attraction, and the system is then forced to re-disintegrate in a ‘fast fission’ process instead of forming a compound nucleus.

In the past twenty years this phenomenon has been illustrated by numerous (classical) dynamical calculations (see for example [8, 9]). Such dynamical models confirm the geometrical interpretation of the entrance channel hindrance, and are even successful in accounting roughly for the critical condition where the hindrance to fusion makes its appearance. But they are unable to give a useful estimate of the hindrance itself. This is because in a classical dynamical calculation the predicted probability to fuse is either one or zero, depending on whether or not the barrier has been overcome. In the past years it has been generally recognized that dynamical calculations have to include statistical fluctuations leading to a diffusion of probabilities in order to have a chance of reproducing data. A large number of such studies is now available (for example [9–14] and the reviews [15, 16] with their numerous references). What I hope to do in this talk is to bring out the basic physics of the observed hindrance, and to estimate its magnitude by an elementary formula. This means that I will focus on the middle one of the three factors that go into an estimate of heavy-element fusion cross sections:

$$\text{Fusion} = (\text{Sticking}) \times (\mathbf{\text{Diffusion}}) \times (\text{Survival}). \quad (1)$$

## 2. An equation for the hindrance factor

In order to illustrate the bare-bones essence of the hindrance phenomenon let us analyze what happens when a system is started off on the ‘wrong’ side of a potential energy barrier, assumed to be in the form of an inverted parabola. (This problem has recently been treated in [12,13] as a special case of a more general formalism.) We shall also assume that the dynamics, including statistical fluctuations, is described by a process analogous to the motion of a swarm of Brownian particles suspended in a fluid at temperature  $T$ . The bulk of the swarm will be sliding down the shoulder of the parabola but, because the swarm’s width increases with time, some of the particles will diffuse ‘up hill’, and a fraction will be able to overcome the barrier and achieve fusion. Can we make an estimate of this fraction?

Let us write the parabolic potential energy as

$$V(x) = -\frac{1}{2}bx^2, \quad (2)$$

where  $x$  is some suitable elongation coordinate. The driving force in the  $x$ -direction is  $bx$ . Let us inject, at time  $t = 0$ , a delta function swarm of Brownian particles at a point  $x_0$ , where the potential is  $-B$ . Thus the barrier height to be overcome by diffusion grows quadratically with  $x_0$  according to:

$$B = \frac{1}{2}bx_0^2. \quad (3)$$

The equation describing the drift and the spreading of the probability distribution  $W(x, t)$  (the probability to find a Brownian particle at position  $x$  at time  $t$ ) is the text-book Smoluchowski diffusion equation (a special case of a Fokker–Planck equation [17]). Allow me to simply write it down for the case of our assumed parabolic potential:

$$G\frac{\partial W}{\partial t} = -(bxW)' + TW'', \quad (4)$$

where primes denote partial differentiations with respect to  $x$ . The first term on the right, containing the driving force  $bx$ , determines the drift, the second, proportional to the temperature  $T$ , determines the spreading of the distribution. The constant  $G$  is a friction coefficient. In the case of Brownian particles it is proportional to the viscosity of the fluid in which the particles are suspended. Very fortunately it will turn out that the fusion probability that we shall derive is *independent* of  $G$ , so we need not say more about the friction coefficient at this stage.

The *exact* solution of Eq. (4) turns out to be a Gaussian whose average position slides towards infinity in the  $x$ -direction, and whose width increases monotonically with time. The fraction  $H$  of particles in the Gaussian distribution that has achieved fusion is equal to the area under the distribution’s

tail in the regime of negative  $x$ -values. This area is readily written down as a function of time, but I shall merely quote the asymptotic result for  $t \rightarrow \infty$ . This gives the theoretical hindrance factor (see Appendix A):

$$H = \frac{1}{2} \operatorname{erfc} \sqrt{\beta} \quad \text{for } x_0 > 0, \quad (5a)$$

$$H = 1 - \frac{1}{2} \operatorname{erfc} \sqrt{\beta} \quad \text{for } x_0 < 0, \quad (5b)$$

where  $\beta = B/T$ , and  $\operatorname{erfc}$  is the error function complement, equal to  $1 - \operatorname{erf}$ . For injection at the top of the barrier (*i.e.*, for  $x_0 = 0$ ,  $B = 0$ ) we have  $H = 0.5$ , as expected by symmetry. For large positive  $x_0$  we find

$$H \approx \frac{1}{\sqrt{4\pi\beta}} \exp(-\beta). \quad (6)$$

For negative  $x_0$  (injection *inside* the barrier)  $H$  tends to unity as  $x_0$  becomes increasingly negative.

Note that the formula for  $H$  is independent of the friction coefficient  $G$ , and that the injection point  $x_0$  and the force constant  $b$  do not enter separately, but only through  $B$ . In the end, the only parameter controlling the fusion probability is the barrier parameter  $B/T$ , *i.e.*, the barrier height (as seen from the injection point) in units of the temperature (assumed independent of  $x$ ). Moreover, with increasing  $x_0$ , the hindrance soon becomes dominated by the familiar Boltzmann factor  $\exp(-B/T)$ . It was not initially obvious that things would turn out that simple because, in contrast to the more familiar *quasi-stationary* situation where a Boltzmann factor controls the slow leakage of probability out of a potential energy hollow, we are now dealing with a *dynamical, non-stationary* system accelerating to infinity in a repulsive field of force.

Owing to the welcome simplicity of Eq. (5) we can now easily translate the experimental hindrance factors  $H$  into barrier parameters  $\beta$ , as shown in Fig. 3. It turns out that for all the reactions in question the injection temperature  $T$  is approximately the same (about 0.6 MeV) so that the principal reason for the increase of the hindrance with atomic number is the increase in the height of the barrier that needs to be overcome 'from outside' in order to reach the compound nucleus configuration. As I mentioned before, this is caused by the shrinking of the saddle point shape, which leaves the injection point increasingly farther from, and lower than, the top of the barrier. This is the so-called 'extra push' phenomenon: in the absence of fluctuations one would need an extra bombarding energy to force a highly charged system dynamically over the barrier. This extra push increases rapidly with atomic number and can assume values much in excess of the barrier  $B$  itself, especially if the dynamics is strongly dissipative [8, 12].

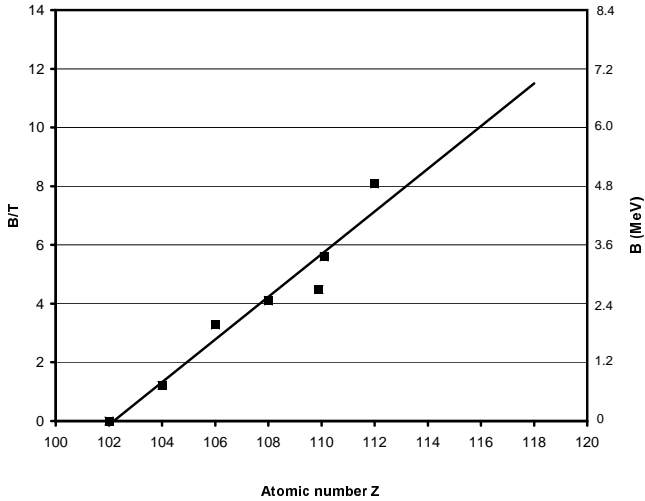


Fig. 3. The barrier factors  $B/T$  obtained by equating the experimental hindrance factors from Fig. 2 to the theoretical Smoluchowski factors  $(1/2)\text{erfc}\sqrt{B/T}$ . The scale on the right gives the resulting barriers obtained by taking 0.6 MeV for the temperature  $T$ .

Up to now all I did was to introduce a little piece of mathematics dealing with diffusion in an idealized parabolic potential in order to convert ‘experimental’ hindrance factors  $H$  into ‘experimental’ barrier parameters  $\beta$ , or barrier heights  $B$  (equal to about  $0.6\beta$  MeV). As you can see from Fig. 3, these barriers range from around zero for  $^{48}\text{Ca} + ^{208}\text{Pb}$  to about 5 MeV for  $^{70}\text{Zn} + ^{208}\text{Pb}$ . Can we account for these values on the basis of some simple model of the fusion process?

### 3. Injection into the asymmetric fission valley

I will try to answer this by using the following picture of the dynamical evolution of the system after contact of target and projectile. It is a familiar everyday observation that after contact of two fluid drops there takes place a sudden neck growth that fills in part of the space between them: the drops get zipped together to form a mononucleus. This happens on a time scale faster than other collective motions, such as the change in the overall length of the configuration. The driving force for this neck zip is the great saving in surface energy counteracted by only small inertial forces associated with minor local rearrangements of the density distribution in the neck region. Let us denote by  $s$  the distance between the half-density surfaces of target and projectile at which the neck zip is assumed to take place. (The value of  $s$  is expected to be in a range determined by the diffuseness of the nuclear

surfaces. For sharp surfaces,  $s$  would be zero.) Instead of trying to follow in detail the dynamics of the neck growth, let us approximate the end result of the zip by a static calculation, in which the potential energy is minimized with respect to the neck size at fixed elongation of the system and at fixed asymmetry. We shall refer to the resulting configuration as lying in the ‘asymmetric fission valley’. Thus we picture the system, originally in the fission valley of two approaching fragments, to be injected into the asymmetric fission valley at a point defined by the initial elongation, the initial asymmetry and by an optimized neck size. (The initial elongation is the sum of the fragment diameters augmented by  $s$ .) The suggested static approximation is not a unique prescription because it depends on the assumed parameterization of the nuclear shapes. In what follows we shall adopt the frequently used parameterization consisting of two spheres connected smoothly by a portion of a hyperboloidal (or spheroidal) neck. Appropriate maps of nuclear deformation energies of such shapes (in a macroscopic approximation) are available in [18]. Using these maps we constructed algebraic expressions (detailed in the Appendix B) for the deformation energy  $V(s)$  along the asymmetric fission valley. Fig. 4 shows these deformation energies for the eight systems under discussion.

Taking the top curve as an example (it refers to the reaction  $^{48}\text{Ca} + ^{208}\text{Pb}$ ) we see that the potential  $V(s)$  is *almost independent* of  $s$  in the range of interest, so that  $B \approx 0$  for any reasonable value of  $s$  at injection. This means that, according to Eq. (5), we expect a hindrance factor of about 0.5. Thus Fig. 4 predicts that, for the sequence of the eight reactions considered, the reaction  $^{48}\text{Ca} + ^{208}\text{Pb}$  marks the approximate point beyond which significant entrance channel hindrances make their appearance. This is a *bona fide* prediction of the neck-zip prescription, obtained without the adjustment of parameters.

At the other extreme, for the reaction  $^{70}\text{Zn} + ^{208}\text{Pb}$ , a choice of  $s \approx 0.5$  fm would reproduce the barrier of about 5 MeV and thus the associated ‘experimental’ hindrance of  $10^{-4.5}$ .

The situation at this stage may be summarized as follows. We have assumed the cross section for fusion to be the product of three factors according to Eq. (1). For the cross section for sticking and for the survival probability we used formulae that work for not too heavy systems. We estimated the theoretical hindrance factor by constructing the potential energy along a (macroscopic) asymmetric fission valley, and assuming that the system is injected into this valley at a point determined by the surface separation parameter  $s$ . This enabled us to calculate the Smoluchowski factor  $(1/2)\text{erfc}\sqrt{\beta}$ . What we get out of this scheme is:

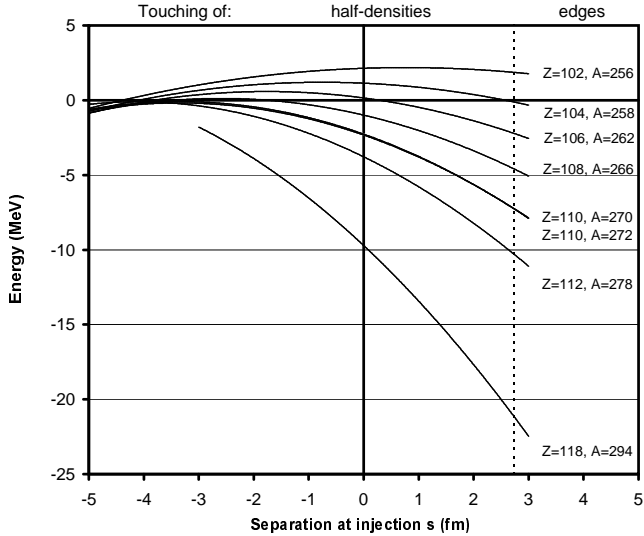


Fig. 4. Macroscopic deformation energies in an asymmetric fission valley obtained by minimizing the energy with respect to neck size at fixed asymmetry and overall length. The nuclear shapes were parameterized as two spheres connected smoothly by a hyperboloid or spheroid according to Ref. [30]. The variable  $s$  is the overall length minus the sum of the diameters of target and projectile. The dashed vertical line shows approximately the value of  $s$  where the semi-classical (Thomas–Fermi) edges of the density distributions touch. The curves with  $s$  less than about  $-1$  fm are extrapolations of uncertain accuracy.

- (1) a prediction of the first appearance of substantial hindrances around the reaction  $^{48}\text{Ca} + ^{208}\text{Pb}$ , and
- (2) an estimate that the hindrance for the reaction  $^{70}\text{Zn} + ^{208}\text{Pb}$  could be accounted for by assuming a value of about  $0.5$  fm for the injection separation  $s$ .

#### 4. Predicted cross sections

Now we can go ahead and calculate the peak cross sections for the eight reactions under consideration, for any given assumption about the value of  $s$  at injection. The upper line in Fig. 5 shows what happens if we take a common value  $s = 0$  for all cases. (This means injection at the contact of the half-density surfaces.) The very poor fit to the data can be improved by taking  $s = 1.2$  fm, but the experimental trend with  $Z$  is still not well reproduced. Motivated by the idea of ‘unshielding’ from [19] we tried a prescription in which the injection distance is taken to be a decreasing function

of  $Z$ . The thick line in Fig. 6 shows the result of assuming  $s$  to decrease linearly from 2.1 fm for  $Z = 102$  to  $-0.3$  fm for  $Z = 118$ . This gives about the optimum fit to the data using a linear dependence of  $s$  on  $Z$ . The implication is that the heavier systems achieve a greater compactness at injection. This is in line with the decreasing role of the Coulomb barrier in shielding the saddle-point configuration from a direct attack by the approaching projectile [19]. Taking the extrapolation of the thick line to  $Z = 118$  at face value, the cross section for the  $^{86}\text{Kr}+^{208}\text{Pb}$  reaction comes out about one order of magnitude below that for  $Z = 112$ . The uncertainties attached to this estimate are very large, at least plus or minus an order of magnitude, as shown by the upper and lower dashed lines in Fig. 6, corresponding to changing the range of  $s$  values from the previous (2.1 fm to  $-0.3$  fm) to either (2.4 fm to  $-0.8$  fm) or (1.8 fm to 0.2 fm). But even these large uncertainties are not the only source of error in estimating cross sections using the scheme outlined above. Further uncertainties are related to the way in which the sticking cross section and the survival probability were estimated. We shall give a brief description of these estimates in what follows. A fuller account is not attempted in the present paper, whose main concern is with the hindrance factors described in terms of a diffusion process.

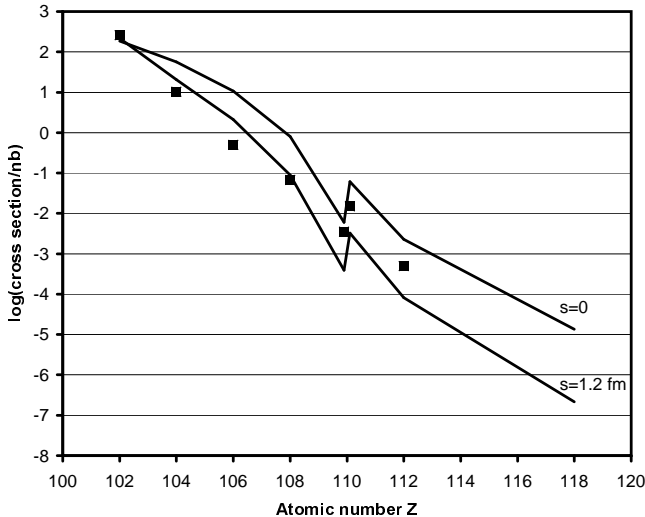


Fig. 5. Comparison of experimental (points) and theoretical (lines) cross sections. The latter were based on assuming injection into the asymmetric fission valley to have taken place either at a surface separation of target and projectile  $s$  equal to zero (the touching of the half-density surfaces), or at a separation  $s = 1.2$  fm.

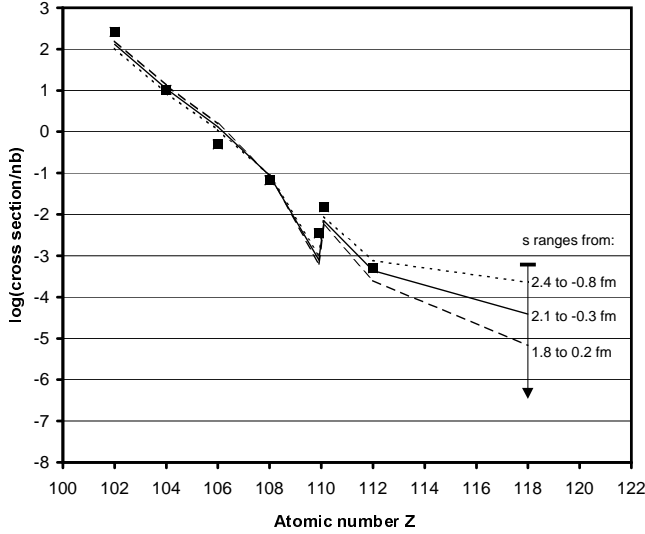


Fig. 6. This is like Fig. 5, but the separation between the surfaces was assumed to decrease linearly with  $Z$ . Three cases are shown, with  $s$  decreasing from 2.4 fm to  $-0.8$  fm, or from 2.1 fm to  $-0.3$  fm, or from 1.8 fm to 0.2 fm between  $Z = 102$  and  $Z = 118$ .

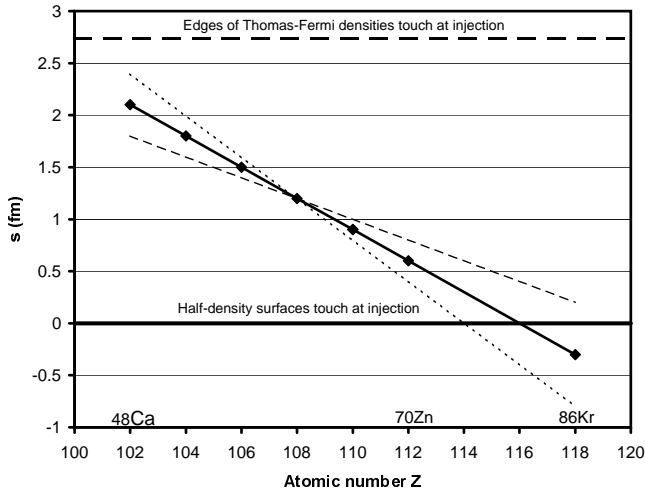


Fig. 7. This figure illustrates the three assumptions about the dependence of the surface separation  $s$  at injection that were used in constructing Fig. 6. It suggests that in the heavier systems injection may be taking place at a more intimate contact of the surfaces, as might be expected from the unshielding hypothesis of Ref. [19].

### 5. Sticking cross section

The sticking or capture cross sections were calculated using the formalism of effective barrier distributions in the version described in [20]. The formula for the cross section reads:

$$\sigma_s = \pi R^2 \frac{w}{E\sqrt{2\pi}} [\sqrt{\pi}X(1 + \operatorname{erf}X) + \exp(-X^2)] , \quad (7)$$

where  $R$  stands for the sum of the target and projectile radii, taken as  $1.27(A_T^{1/3} + A_P^{1/3})$  fm, and where  $X = (E - V)/w\sqrt{2}$ , with  $V$  equal to the mean and  $w$  the width (the square root of the variance) of the distribution of barrier heights (assumed Gaussian) on which Eq. (7) is based. The values of  $V$  and  $w$  were calculated using the systematics described in Ref. [20], and are listed in Table II.

TABLE II

Mean barrier  $V$  and width  $w$  used in Eq. (7).

Reaction	Mean Barrier $V$ (MeV)	Width $w$ (MeV)
$^{48}\text{Ca} + ^{208}\text{Pb}$	178.1	3.24
$^{50}\text{Ti} + ^{208}\text{Pb}$	198.6	4.72
$^{54}\text{Cr} + ^{208}\text{Pb}$	218.3	5.96
$^{58}\text{Fe} + ^{208}\text{Pb}$	238.4	7.30
$^{62}\text{Ni} + ^{208}\text{Pb}$	258.8	8.71
$^{64}\text{Ni} + ^{208}\text{Pb}$	257.4	8.25
$^{70}\text{Zn} + ^{208}\text{Pb}$	276.7	9.47
$^{86}\text{Kr} + ^{208}\text{Pb}$	337.8	13.13

Equation (7) gives a fair account of the capture cross sections for about 50 reactions listed in Refs. [20, 21], but extrapolation to still heavier systems is, naturally, subject to considerable uncertainty.

### 6. The survival probability

We used the canonical transition state theory of reaction rates to calculate the probability for the compound nucleus to survive fission. Consider the compound nucleus with mass number  $A$  formed in a collision with center of mass energy  $E$ . Let the mass of the saddle point for fission — the fission transition state — be  $V_f$  in energy units, as measured *with respect to the sum of the target and projectile masses*. (We take this as our reference baseline rather than the mass of the ground state of the compound nucleus, because the latter is often not known experimentally for the very heavy nuclei in

question, and this introduces a spurious uncertainty in the analysis.) Let  $V_n$  stand for the mass of the transition state for neutron emission (taken with respect to the above baseline). This is the mass of the residual nucleus ( $A - 1$ ) in its ground state plus the mass of a neutron minus the sum of the ground state masses of the target and projectile. According to the transition state theory of reaction rates (see, for example, Ref. [22]) the ratio of neutron to fission disintegration widths is given by

$$\frac{\Gamma_n}{\Gamma_f} = \frac{N_n}{N_f} = \frac{\int_0^{U_n} \rho_n(\varepsilon) d\varepsilon}{\int_0^{U_f} \rho_f(\varepsilon) d\varepsilon}, \quad (8)$$

where  $N_n$  and  $N_f$  are the numbers of states (channels) of the neutron and fission transition states in the intervals  $U_n = E - V_n$  and  $U_f = E - V_f$ , respectively. Expressing the level density  $\rho(\varepsilon)$  in terms of the exponential of the entropy  $S(\varepsilon)$ , and using the standard approximation to evaluate the integrals by an expansion of the integrand about the upper limit, we find the result

$$\frac{\Gamma_n}{\Gamma_f} = \frac{S'_f}{S'_n} \exp(S_n - S_f), \quad (9)$$

where  $S_n$  and the derivative  $S'_n$  (the inverse of temperature) are evaluated at  $U_n$ , and  $S_f$  and  $S'_f$  are evaluated at  $U_f$ . We used formulae for the entropies that include corrections for shell and pairing effects, as well as for the dependence of the level densities on nuclear shape (Appendix C).

The probability for the compound nucleus to emit a neutron rather than fission is now given by  $\Gamma_n/\Gamma_t$ , where  $\Gamma_t = \Gamma_n + \Gamma_f$ . After this emission, the nucleus must neither fission nor emit a second neutron. For this to be the case the first neutron must have carried off sufficient energy to bring the system below the thresholds for neutron emission and fission. (We neglect sub-barrier fission on the one hand and, on the other, gamma emission at excitation energies above the fission barrier.) In the case of the eight reactions in question the threshold for emitting a second neutron is always higher than the threshold for fission. We denote the latter by  $V_f^{A-1}$ , equal to the mass of the fission transition state of the residual nucleus ( $A - 1$ ) plus the mass of a neutron minus the sum of the ground state masses of target and projectile. The energy available to overcome this fission threshold is  $E - K$ , where  $K$  is the kinetic energy of the originally emitted neutron. If  $E < V_f^{A-1}$ , there is no restriction on the possible values of  $K$ . But if  $E > V_f^{A-1}$  then, in order to prevent fission, we must have  $K > K_1$ , where

$$K_1 = E - V_f^{A-1}. \quad (10)$$

Using a Maxwellian distribution of the neutron's kinetic energies, proportional to  $K \exp(-K/T)$ , where  $T$  is the temperature of the neutron transition state, we find for the probability that  $K > K_1$  the expression  $(1 + K_1) \exp(-K_1/T)$ . Hence the final expression for the probability for the compound nucleus to survive fission and emit just one neutron is

$$P(E) = \frac{\Gamma_n}{\Gamma_t}, \quad \text{if } E < V_f^{A-1}, \quad (11a)$$

$$P(E) = \frac{\Gamma_n}{\Gamma_t} (1 + K_1) \exp(-K_1/T), \quad \text{if } E > V_f^{A-1}. \quad (11b)$$

### 7. Theoretical excitation functions

The product of the above expressions for  $\sigma_s(E)$  and  $P(E)$  gives the theoretical excitation function for the reaction in question in the absence of any hindrance. An example is shown in Fig. 8. The dashed line indicates the average of the excitation function, and the point with the nominal 0.5 MeV horizontal error bar indicates the position of the average of the experimental excitation function deduced from Fig. 19 in Ref. [1].

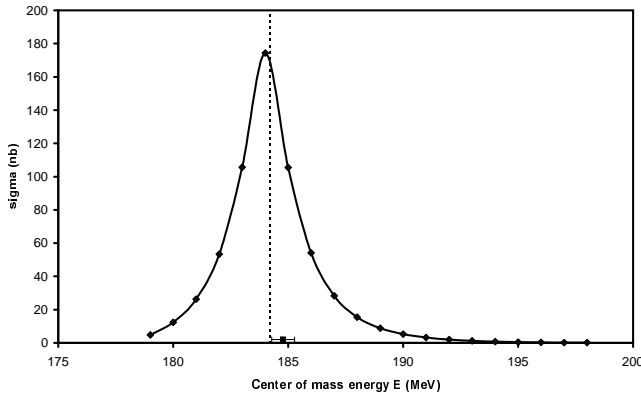


Fig. 8. The excitation function for the reaction  $^{50}\text{Ti} + ^{208}\text{Pb}$  as calculated using Eqs. (7) and (11) in the text. The average (a little higher than the maximum) is indicated by the dashed line. The point with a nominal 0.5 MeV error bar locates the maximum of the experimental excitation function. The predicted theoretical excitation function would be obtained with fair approximation by multiplication by the theoretical hindrance factor *at the maximum*, because the energy dependence of the Smoluchowski factor (entering through the temperature  $T$ ) is rather slight in the range of energies of interest.

The qualitative appearance of such excitation functions is readily accounted for. When  $E < V_f^{A-1}$  the cross section is dominated by the steeply increasing function  $\sigma_s(E)$ . (In the cases under consideration, the energy  $E$  is well below the mean barrier position  $V$  in Eq. (7), in the ‘sub-barrier’ regime of the explosively growing tail of  $\sigma_s(E)$ .) This increase continues up to  $E = V_f^{A-1}$ , after which it is very soon reversed by the even more steeply *decreasing* function  $P(E)$ , whose characteristic fall-off range is equal to the temperature  $T_n$  of the neutron transition state, a mere 0.4 to 0.6 MeV. The result is a sharply peaked excitation function with a maximum a little (about 0.5 MeV) above  $V_f^{A-1}$  and a narrow width. The decrease of  $P$  is so abrupt — almost razor sharp — that, at the maximum, the actual cross section has not had a chance to decrease much below its former trend. This is illustrated in Table I, where the values of  $\Gamma_n/\Gamma_t$  and  $P$  hardly differ, and in two cases are actually equal. (That this latter result is not an error is explained by the fact that the values listed in Table I are not true maxima, but *the highest* values found in a scan in steps of 1 MeV.) Note the interesting insight that emerges from the above mentioned interpretation, namely that the bombarding energy associated with the sudden downturn in the cross section, when added to the masses of the fragments at infinity, leads to an almost direct determination of the saddle point mass of the nucleus ( $A - 1$ ). Conversely, if the mass of the saddle point is known, or can be estimated, we arrive at the following “Optimum energy rule”:

*“The optimum center-of-mass bombarding energy in a one-neutron-out heavy ion reaction is approximately equal to the mass of the fission saddle point of the residual nucleus plus the mass of a neutron minus the masses of target and projectile plus about 0.5 MeV:  $E_{CM} \approx M_{SP} + M_n - M_T - M_P + 0.5 \text{ MeV}$ ”.*

Here is how it works in the case of the reaction  $^{50}\text{Ti} + ^{208}\text{Pb} \rightarrow ^{258}\text{Rf}$ . Using mass excesses instead of masses, we have: measured mass excess of ground state of  $^{257}\text{Rf} = 96.01 \text{ MeV}$ ; fission barrier in  $^{257}\text{Rf}$  (assumed the same as in  $^{258}\text{Rf}$ ) = 6.39 MeV (Appendix C); mass excess of saddle point of  $^{257}\text{Rf} = 102.40 \text{ MeV}$ ; mass excess of neutron 8.07 MeV; sum of mass excesses of target and projectile =  $-73.20 \text{ MeV}$ . It follows that the expected downturn in the excitation function should be close to  $E = 102.40 + 8.07 + 73.20 + 0.5 = 184.17 \text{ MeV}$ . This agrees with the theoretical curve in Fig. 8, and is a little lower than the measured maximum at about 184.8 MeV. (A small difference with this sign could be due to gamma emission competing successfully with fission just above the nominal threshold, so that the *effective* threshold for fission would be a little higher than  $V_f^{A-1}$ .)

An alternative way of making the above estimate is to rely on the “topographic theorem” (described in Appendix C of Ref. [23]) and to assume that the effect of shell structure on the saddle point energy is negligible, so

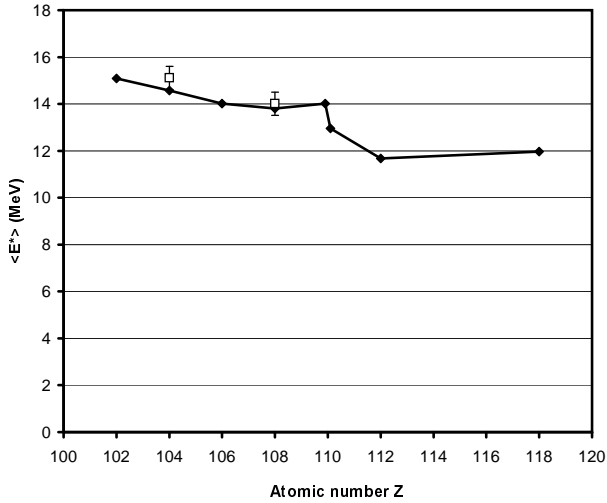


Fig. 9. The calculated average values  $\langle E^* \rangle$  of the excitation functions are plotted against  $Z$  for the eight reactions under study. After a slight decrease from about 15 MeV to 12 MeV between  $Z = 102$  and  $Z = 112$ , the calculations show a leveling off at  $Z = 118$ . The two available measurements are shown with nominal error bars of  $\pm 0.5$  MeV.

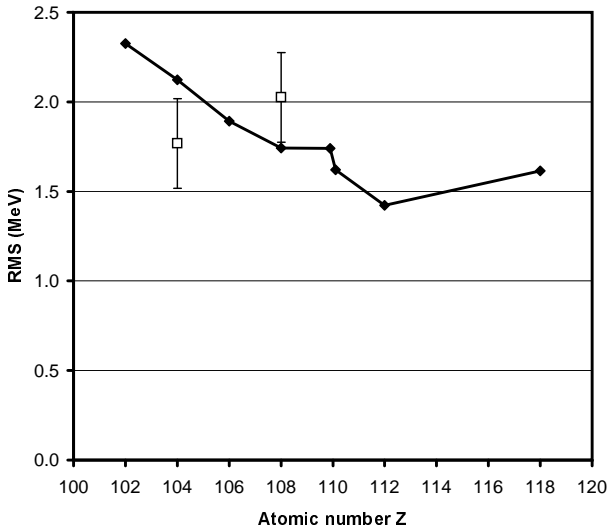


Fig. 10. A comparison of the calculated and measured RMS widths of excitation functions. The former show a systematic decrease between  $Z = 102$  and  $Z = 112$ , followed by a slight rise at  $Z = 118$ . A correction for energy dispersion in the target has not been included in the theoretical widths.

that the use of a macroscopic estimate of the saddle point mass is adequate. We now have the following numbers: macroscopic mass excess of spherical  $^{257}\text{Rf} = 101.15$  MeV (from Ref. [24]); macroscopic fission barrier = 0.76 MeV (this follows from the liquid drop approximation: barrier =  $(98/135)E_s(1-x)^3$ , where formulae for the surface energy  $E_s$  and the fissility  $x$  are given in Appendix B); hence mass excess of saddle point of  $^{257}\text{Rf} = 101.91$  MeV, and the maximum of the excitation function should be about 183.68 MeV, *i.e.*, 0.49 MeV below the previous estimate.

Fig. 9 shows the calculated average positions of the excitation functions, and Fig. 10 their RMS widths for the eight reactions under discussion. The two experimental points refer to  $^{50}\text{Ti} + ^{208}\text{Pb}$  and  $^{58}\text{Fe} + ^{208}\text{Pb}$ , the only cases out of the eight for which the excitation functions had been approximately established.

## 8. Summary and conclusion

We have outlined a theory of fusion cross sections for very heavy systems in terms of the product of three factors: a sticking cross section, a Smoluchowski factor  $(1/2)\text{erfc}\sqrt{\beta}$  and a survival probability. The first and third correspond more or less to standard treatments that, on a logarithmic scale, reproduce very well fusion cross sections for not too heavy systems. The middle one is based on the Smoluchowski diffusion equation in an inverted parabolic potential. This potential was estimated using a macroscopic deformation energy in an asymmetric fission valley. For a given reaction there is in this scheme one adjustable parameter,  $s$ , the point of injection into the above valley. We found that the values of  $s$  that reproduce the order of magnitude of the experimental cross sections are in the range expected on physical grounds. This range is determined by the nuclear surface diffuseness, and spans approximately situations intermediate between the contact of the half-density surfaces and the contact of the semi-classical, *i.e.* Thomas–Fermi, edges of the density distributions. Pressing the fit of theory to data beyond a qualitative correspondence, there is an indication for a need to make the value of  $s$  at injection a *decreasing* function of  $Z$ . This is in line with the expectation of an unshielding of the saddle point configuration caused by the lowering of the Coulomb barrier relative to the saddle-point energy. It remains to be seen whether this is the correct interpretation of the overall trend of the measured cross sections. A closer look at the energy dependence of the theoretical cross sections leads to a useful insight regarding the optimum bombarding energies for fusion (the ‘optimum energy rule’) and the expected RMS widths of the excitation functions. Note that these results depend only on the first and third factors in Eq. (1). They provide what appears to be quite precise determinations of two out of the three cru-

cial quantities needed in planning heavy element production experiments, and are not subject to the uncertainties associated with the diffusion factor. The latter is needed only to establish the *absolute magnitudes* of the cross sections, which is the third important characteristic of a reaction.

There are, indeed, reasons for being cautious about the significance of our estimates of the absolute magnitudes of the cross sections, deduced as they are from a very idealized theory, adjusted to data by an assumption concerning the separation  $s$  at injection. A large number of approximations were introduced in formulating the model, too numerous for a detailed discussion here. To single out an important one: our macroscopic deformation energies neglect shell effects, except as these are reflected in the ground states of the target, projectile and the compound nucleus. We may take some comfort in the observation that, for the reactions in question, the observed cross sections are fairly smooth functions of  $Z$  (except for a glitch between  $^{270}\text{110}$  and  $^{272}\text{110}$ ). The fact that a smooth macroscopic treatment is able to reproduce them (including the glitch!) is some indication that at least the *variations* in the neglected shell effects in going from  $^{48}\text{Ca}$  to  $^{70}\text{Zn}$  projectiles are not very significant. On the other hand, the shell effect associated with  $^{208}\text{Pb}$  is expected to be important, and is likely to have affected significantly the values of  $s$  deduced from the data.

Looking towards the future, an obvious extension of the present work is the application to other reactions, in the first place those using a bismuth target. Inclusion of reactions where more than one neutron is emitted will be another test of the self-consistency of the model and of its range of applicability.

We would like to thank W.D. Myers for many unpublished results obtained with the Thomas–Fermi model and used in this paper, and R. Smolańczuk for information on microscopic fission barriers and saddle-point deformations. One of us (W.J.S.) thanks J. Randrup for an illuminating discussion concerning diffusion equations. This work was supported in part by the Poland USA Maria Skłodowska-Curie Joint Fund II, under project No. PAA/DOE-98-34, and by the D.O.E. under contract No. DE-AC03-76SF00098 (LBNL). One of us (J.W.) acknowledges support by the Polish State Committee for Scientific Research (KBN), Grant No. 2P03B05419.

## Appendix A

Introducing a dimensionless time by  $\tau = t/t_0$ , where  $t_0 = G/b$ , Eq. (4) in the text becomes

$$\frac{\partial W}{\partial \tau} = -(xW)' + \theta W'', \quad (\text{A.1})$$

where  $\theta = T/b$ . It may then be verified by direct substitution that the solution of Eq. (A.1), with the initial condition that  $W$  is a  $\delta$ -function at  $x = x_0, t = 0$ , is given by

$$W(x, \tau) = \frac{1}{\sqrt{2\pi\Sigma}} \exp\left(-\frac{(x - x_0 \exp \tau)^2}{2\Sigma}\right), \quad (\text{A.2})$$

where  $\Sigma = \theta(\exp 2\tau - 1)$ .

Integrating Eq. (A.2) from  $x = -\infty$  to  $x = 0$  and taking the limit  $\tau \rightarrow \infty$ , gives Eq. (5) in the text. We note in passing that if at  $t = 0$  we postulate as the initial condition a Gaussian distribution with variance  $\sigma$ , *i. e.*,

$$W(x_0, 0) = \frac{1}{\sqrt{2\pi\sigma}} \exp\left(-\frac{(x - x_0)^2}{2\sigma}\right), \quad (\text{A.3})$$

the solution of Eq. (A.1) is still of the form of Eq. (A.2), but with the variance  $\Sigma$  now given by

$$\Sigma = \sigma \exp 2\tau + \theta(\exp 2\tau - 1). \quad (\text{A.4})$$

The expression for the resulting hindrance factor is still of the form of Eq. (5), but with  $T$  replaced by  $T = T + b\sigma$ .

### Appendix B

The following formulae provide approximations to the macroscopic deformation energy  $\Delta E$  of a nucleus idealized as a uniformly charged liquid drop. The shape of the drop, originally spherical with radius  $R$ , is parameterized by two spheres connected smoothly by a portion of a spheroid or hyperboloid [30]. Three variables specify a given shape: elongation, asymmetry and neck size.

Let  $\xi$  denote the deformation energy in units of the surface energy  $E_s$  of the spherical shape. Let  $\sigma$  stand for the surface-separation variable  $s$  in units of  $R$ . (This  $\sigma$  should not be confused with the  $\sigma$  in Appendix A.) Recall that  $s$  is the excess of the overall length  $L$  of the shape in question over the sum of the diameters of target and projectile. Thus

$$s = L - 2(R_T + R_P), \quad \sigma = \frac{s}{R}, \quad \xi = \frac{\Delta E}{E_s}. \quad (\text{B.1})$$

For each value of  $s$ , the energy is considered to have been minimized with respect to the neck variable at fixed asymmetry. The resulting deformation energy is consequently a function of the single variable  $s$ . In a range of parameters to be specified later, a quadratic approximation to  $\xi(\sigma)$  is adequate:

$$\xi \approx a + b\sigma + c\sigma^2. \quad (\text{B.2})$$

The coefficients  $a$ ,  $b$ ,  $c$  are functions of the asymmetry variable  $\Delta$  and of the fissility  $x$  defined as follows:

$$\Delta = \frac{R_T - R_P}{R_T + R_P}, \quad (\text{B.3})$$

$$x = \frac{\text{Electrostatic energy of sphere}}{2E_s}. \quad (\text{B.4})$$

Using the notations  $D = \Delta^2$  and  $t = 1 - x$ , we have

$$a = \alpha_a + \beta_a t + \gamma t^2, \quad (\text{B.5})$$

$$b = \alpha_b + \beta_b t, \quad (\text{B.6})$$

$$c = \alpha_c + \beta_c t, \quad (\text{B.7})$$

where

$$\alpha_a = -0.00557 - 0.01929 \exp(-D/0.02283), \quad (\text{B.8})$$

$$\beta_a = 0.048 + 0.12151 \exp(-D/0.04053), \quad (\text{B.9})$$

$$\gamma = -0.073 + 0.94D, \quad (\text{B.10})$$

$$\alpha_b = -0.00858 - 0.05303 \exp(-D/0.03205), \quad (\text{B.11})$$

$$\beta_b = 0.019 + 0.25663 \exp(-D/0.07331), \quad (\text{B.12})$$

$$\alpha_c = -0.0256 + 0.1944D, \quad (\text{B.13})$$

$$\beta_c = 0.0214 + 0.6158D. \quad (\text{B.14})$$

The above formulae have been tested for adequate accuracy in the range  $0.85 < x < 1.05$ ,  $-0.25 < \Delta < 0.25$  and  $-0.1 < \sigma < 0.44$ .

In order to convert the dimensionless quantities into MeV, the following equations should be used:

$$E_s = 17.9439(1 - 1.7826I^2)A^{2/3} \text{MeV}, \quad (\text{B.15})$$

$$x = \frac{Z^2/A}{50.883(1 - 1.7826I^2)}, \quad (\text{B.16})$$

where  $I = (N - Z)/A$ .

To convert dimensionless lengths into fm use  $R = 1.155A^{1/3}$  fm.

### Appendix C

We used the following expression for  $S_n(U_n)$ , based on Refs. [25, 26]:

$$S_n(U_n) = 2\sqrt{a_n\{U_n^* + \text{SH}[1 - \exp(-U_n^*/k)]\}}, \quad (\text{C.1})$$

where  $U_n^* = U_n - 12\text{MeV}/\sqrt{A-1}$  (for the odd mass numbers  $A-1$ ),  $k = A^{1/3}/0.47$  MeV, and SH is the shell effect, in MeV, in the ground state of nucleus ( $A-1$ ), as given in Refs. [24,27],  $U_n$  is the excitation energy given by  $E - V_n$ , and the level density parameter  $a_n$  was taken as

$$a_n = 0.076(A-1) + 0.180(A-1)^{2/3}F(\alpha_n) + 0.157(A-1)^{1/3}G(\alpha_n) \text{ MeV}^{-1}. \quad (\text{C.2})$$

The last two terms allow approximately for the dependence of the level density on the deformation of the nucleus, as specified by the parameter  $\alpha$ , defined by  $\alpha = (R_{\text{max}} - R)/R$ , where  $R_{\text{max}}$  is the semi-major axis of the (axially symmetric) nucleus (of radius  $R$  before deformation). The functions  $F$  and  $G$  were chosen to be given by

$$F(\alpha) = 1 + (0.6416\alpha - 0.1421\alpha^2)^2, \quad (\text{C.3})$$

$$G(\alpha) = 1 + (0.6542\alpha - 0.0483\alpha^2)^2. \quad (\text{C.4})$$

They reproduce closely, for  $\alpha < 1$ , the relative surface area and integrated curvature for the *symmetric* saddle point shapes in Table 7.1 of Ref. [30], and may be expected to give at least an approximate representation of the corrections for the asymmetric shapes with which we are concerned.

For the entropy  $S_f(U_f)$  we used the expression

$$S_f(U_f) = 2\sqrt{a_f U_f^*}, \quad (\text{C.5})$$

where

$$U_f^* = U_f - 24\text{MeV}/\sqrt{A} \quad (\text{for even-even compound nuclei}), \quad (\text{C.6})$$

$$U_f = E - V_f. \quad (\text{C.7})$$

The level density parameter  $a_f$  was taken according to Eq. (C.2), using the appropriate mass number and deformation for the transition state for fission.

Originally two sets of values of  $V_f$  and  $V_f^{A-1}$  were studied. The first assumed that shell effects at the saddle point were negligible (see the ‘‘Topographic theorem’’ in [23]), and the macroscopic Thomas–Fermi barrier calculations of [28] were used to determine  $V_f$ . The second took account of possible deviations from this idealized limit, for which there is, in fact, empirical evidence in Fig. 4 in Ref. [28]. The Hartree–Fock calculations of Ref. [29] also suggest related deviations between the fission barriers calculated microscopically and those using the macroscopic Thomas–Fermi saddle point energies and a shell-corrected ground state. Thus, for the eight compound nuclei in question, the comparison of calculated fission barriers (in MeV) looks like this: Hartree–Fock/Thomas–Fermi/Difference = 7.23/5.44/1.79;

6.87/5.22/1.65; 6.30/5.08/1.22; 5.70/4.89/0.81; 4.88/4.34/0.54; 5.56/4.53/1.03; 4.05/4.28/−0.23; 5.45/5.57/−0.12. If the differences were ascribed entirely to shell effects at the saddle, the values of  $V_f$  would be correspondingly affected. In the end we adopted a prescription in which the values of  $V_f$  were taken to be a weighted average of the Hartree–Fock and Thomas–Fermi numbers, with a weight of 0.7 for the former and 0.3 for the latter. This weighting ensures that the hindrance factor for the  $^{48}\text{Ca}$  reaction is about 0.5, in agreement with the expectation based on Fig. 4. For reactions with progressively heavier projectiles, the differences between the two ways of estimating  $V_f$  become insignificant.

## REFERENCES

- [1] S. Hofmann, *Rep. Prog. Phys.* **61**, 639 (1998).
- [2] S. Hofmann, F.P. Hessberger D. Ackermann, G. Münzenberg, S. Antalic, P. Cagarda, B. Kindler, J. Kojucharova, M. Leino, B. Lommel, R. Mann, A.G. Popeko, S. Reshitko, S. Šaro, J. Uusitalo, A.V. Yeremin, *Eur. Phys. J.* **A14**, 147 (2002).
- [3] H. W. Gäggeler, D.T. Jost, A. Türler, P. Armbruster, W. Brüche, H. Folger, F.P. Hessberger, S. Hofmann, G. Münzenberg, V. Ninov, W. Reisdorf, M. Schädel, K. Sümmerer, J.V. Kratz, U. Scherer, M.E. Leino, *Nucl. Phys.* **A502**, 561c (1989).
- [4] K.E. Gregorich, T.N. Ginter, W. Loveland, D. Petersen, J.B. Patin, C.M. Folden III, D.C. Hoffman, D.M. Lee, H. Nitsche, J.P. Omvedt, L.A. Omvedt, L. Stavsetra, R. Sudowe, P.A. Wilk, P.M. Zielinski, K. Alklett, submitted to *Eur. Phys. J. A*.
- [5] W.J. Swiatecki, *Phys. Scr.* **24**, 113 (1981).
- [6] W.J. Swiatecki, *Nucl. Phys.* **A376**, 275 (1982).
- [7] S. Bjørnholm, W. J. Swiatecki, *Nucl. Phys.* **A391**, 471 (1982).
- [8] J.P. Blocki, H. Feldmeier, W.J. Swiatecki, *Nucl. Phys.* **A459**, 145 (1986).
- [9] J. Błocki, O. Mazonka, J. Wilczyński, Z. Sosin, A. Wieloch, *Acta Phys. Pol. B* **31**, 1513 (2000).
- [10] Y. Abe, C. Grégoire, H. Delagrangé, *J. Phys.* **47**, C4 (1986).
- [11] P. Fröbrich, S.Y. Yu, *Nucl. Phys.* **A477**, 143 (1988).
- [12] Y. Abe, *Eur. Phys. J.* **A13**, 143 (2002).
- [13] Y. Abe, D. Boilley, B. Giraud, T. Wada, *Phys. Rev.* **E61**, 1125 (1999).
- [14] G. Giardina, S. Hofmann, A.J. Muminov, A.K. Nasirov, *Eur. Phys. J.* **A8**, 205 (2000).
- [15] P. Armbruster, *Rep. Prog. Phys.* **62**, 465 (1999).
- [16] P. Fröbrich, I.I. Gonchar, *Phys. Rep.* **292**, 131 (1998).
- [17] H. Risken, *The Fokker-Planck Equation*, Springer-Verlag, 1989.

- [18] J. Błocki, W. J. Świątecki, *Nuclear Deformation Energies*, Lawrence Berkeley Laboratory preprint LBL-12811, May 1982, unpublished.
- [19] W.D. Myers, W.J. Świątecki, *Acta Phys. Pol. B* **31**, 1471 (2000); **32**, 1033 (2001).
- [20] K. Siwek-Wilczyńska, E. Siemiaszko, J. Wilczyński, *Acta Phys. Pol. B* **33**, 451 (2002).
- [21] K. Siwek-Wilczyńska, J. Wilczyński, *Phys. Rev.* **C64**, 024611 (2001).
- [22] W.J. Swiatecki, *Aust. J. Phys.* **36**, 641 (1983).
- [23] W.D. Myers, W.J. Swiatecki, *Nucl. Phys.* **A601**, 141 (1996).
- [24] W.D. Myers, W.J. Swiatecki, *Table of Nuclear Masses According to the 1994 Thomas-Fermi Model*, Lawrence Berkeley Laboratory preprint LBL-36803, December 1994, also available by “anonymous” ftp at [www-nsdth.lbl.gov](http://www-nsdth.lbl.gov) in the directory pub/myers.
- [25] A.V. Ignatyuk, G.N. Smirenkin, A.S. Tishin, *Sov. J. Nucl. Phys.* **29**, 255 (1975).
- [26] S.F. Mughabghab, C. Dunford, *Phys. Rev. Lett.* **81**, 4083 (1998).
- [27] P. Möller, J.R. Nix, W.D. Myers, W.J. Swiatecki, *Atomic Data and Nuclear Data Tables*, **59**, 185 (1995).
- [28] W.D. Myers, W.J. Świątecki, *Phys. Rev.* **C60**, 014606 (1999).
- [29] R. Smolańczuk, private communication, 1999.
- [30] R.W. Hasse, W.D. Myers, *Geometrical Relationships of Macroscopic Nuclear Physics*, Springer-Verlag, 1988.